BASIC SCIENCE

Nanomedicine: Nanotechnology, Biology, and Medicine
11 (2015) 1417–1423

Review Article

nanomedjournal.com

Highly bactericidal Ag nanoparticle films obtained by cluster beam deposition

Emanuele Cavaliere, Ph.D.[a], Sebastiano De Cesari, M.S.[a], Giulia Landini, MS[b], Eleonora Riccobono, Ph.D.[b], Lucia Pallecchi, Ph.D.[b], Gian Maria Rossolini, M.D.[b,c], Luca Gavioli, Ph.D. Physics[a,*]

[a]*Interdisciplinary Laboratories for Advanced Material Physics (i-LAMP) & Dipartimento di Matematica e Fisica, Università Cattolica del Sacro Cuore di Brescia, Brescia, Italy*

[b]*Dipartimento di Biotecnologie Mediche, Università degli Studi di Siena, Policlinico Santa Maria alle Scotte, Siena, Italy*

[c]*Dipartimento di Medicina Sperimentale e Clinica, Università di Firenze & SOD Microbiologia e Virologia, Azienda Ospedaliera Universitaria Careggi, Firenze, Italy*

Received 4 December 2014; accepted 28 February 2015

Abstract

The recent emergence of bacterial pathogens resistant to most or all available antibiotics is among the major global public health problems. As indirect transmission through contaminated surfaces is a main route of dissemination for most of such pathogens, the implementation of effective antimicrobial surfaces has been advocated as a promising approach for their containment, especially in the hospital settings. However, traditional wet synthesis methods of nanoparticle-based antimicrobial materials leave a number of key points open for metal surfaces: such as adhesion to the surface and nanoparticle coalescence. Here we demonstrate an alternative route, i.e. supersonic cluster beam deposition, to obtain antimicrobial Ag nanoparticle films deposited directly on surfaces. The synthesized films are simple to produce with controlled density and thickness, are stable over time, and are shown to be highly bactericidal against major Gram positive and Gram negative bacterial pathogens, including extensively drug-resistant strains.

From the Clinical Editor: The use of silver nanoparticle in health care is getting more widespread. The authors here describe the technique of cluster beam deposition for spraying silver on surfaces used in health care sectors. This may open a new avenue for future anti-bacterial coatings.

Key words: Ag nanoparticle-based antimicrobial films; Supersonic cluster beam deposition; Atomic force microscopy; Electron spectroscopies; Bactericidal activity; Extensively drug-resistant bacteria

Backgrounds

Nanoparticles (NPs) are promising alternatives to conventional materials in many branches of science and technology[1-3] since the nanoscale allows to access physical properties and functionalities that often differ significantly from their bulk counterparts. As an example, the antimicrobial activity of nanomaterials such as fullerenes, TiO_2, and Ag NPs has a wide range of important applications in medicine, water disinfection, and consumer products (e.g. cosmetics, laundry detergents, toys, accessories).[3-6] In this scenario, a current challenge is the synthesis and application of NPs[7-9] to implement effective control measures to reduce the incidence of healthcare-associated infections (HAIs). HAIs have become a global threat due to the emergence and dissemination of microbial pathogens that are resistant to most or even all antimicrobial agents available for their treatment (extensively drug-resistant or totally drug-resistant phenotypes).[10,11] HAIs are in fact a major cause of patient morbidity and mortality.[12] Most of the principal nosocomial pathogens can asymptomatically colonize the human host, with colonization representing either a risk factor for infection or a key step for their dissemination. Indeed,

Abbreviations: NP, nanoparticle; HAI, healthcare-associated infection; SCBD, supersonic cluster beam deposition; AFM, atomic force microscopy; XPS, X-ray photoemission spectroscopy; XRD, X-ray diffraction; CFU, colony forming units; ME, microbicidal effect.

The authors declare no competing financial interests.

The authors disclose any commercial associations, current and within the past five years, that might pose a potential, perceived or real conflict of interest to this work. This research was supported in part by Università Cattolica del Sacro Cuore through D2.2 grants.

*Corresponding author. Interdisciplinary Laboratories for Advanced Material Physics (i-LAMP) & Dipartimento di Matematica e Fisica, Università Cattolica del Sacro Cuore di Brescia, Brescia, Italy.

E-mail address: luca.gavioli@unicatt.it (L. Gavioli).

http://dx.doi.org/10.1016/j.nano.2015.02.023

Please cite this article as: Cavaliere E, et al, Highly bactericidal Ag nanoparticle films obtained by cluster beam deposition. *Nanomedicine: NBM* 2015;11:1417-1423, http://dx.doi.org/10.1016/j.nano.2015.02.023

an estimated 20% to 40% of HAIs have been attributed to cross infection via the hands of healthcare personnel, who may become contaminated indirectly by touching contaminated environmental surfaces.[13] Besides the strict adhesion to hand-hygiene practices and classical environmental cleaning procedures, the development of antimicrobial surfaces/coatings characterized by a long-lasting microbicidal effect to be applied in high-touch hospital devices (e.g. buttons or handles), has been advocated as a promising approach.[11,13] Some of the challenging aspects concerning fabrication of antimicrobial films are the adhesion to metal surfaces, determined by the NP–surface interactions, the ability to maintain the microbicidal effect over time and the lack of non-wet synthesis methods.

Among the large number of NPs investigated so far for antimicrobial features, Ag NPs have been considered the most promising ones for potential medical applications.[5] Ag NPs exert an antibacterial activity through a multifactorial process which has not been clearly elucidated, and involving either damaging of bacterial cell wall and plasma membrane, or inhibition of DNA replication and protein synthesis.[14] NP morphological characteristics (i.e. shape, size) have been proven to affect antibacterial efficacy of Ag NPs, with a recent work demonstrating that this could be related to a differential release of Ag^+ ions (i.e. the actual effectors of bactericidal activity).[8]

To date, the synthesis of Ag NPs is largely based on wet chemical reduction starting from a molecular precursor containing Ag in an oxidized state.[15] Such methods allow a great control over size and shape of the Ag NPs, but pose several problems such as the use of colloidal stabilizers, the presence of impurities, the solvents and synthesis process costs to reduce or avoid the problem of NP aggregation in solution.[16,17] Moreover, the mere synthesis of the Ag NPs does not imply a good adhesion of the obtained NPs to the substrate of need. The layer-by-layer approach[16] has been proposed to obtain surfaces on which thin films/layers of Ag NPs are deposited or formed as a molecular self-assembled monolayer, while pre-functionalization of glass has been used to stabilize the Ag NPs on the surface, further complicating the synthesis and deposition process.[17]

A so far unexplored alternative route to Ag NP wet synthesis is provided by the supersonic cluster beam deposition (SCBD).[18,19] The source is based on the pulsed plasma ablation of the material to be deposited and the subsequent formation of an NP beam. The method, which is intrinsically environmentally-friendly since it does not employ solvents, has also been shown to produce NPs with mixed chemical composition,[19] hence allowing the possibility of combining different elements to engineer the material properties. To our knowledge, this method has not been applied yet to synthesize Ag NP films with antimicrobial properties. In the present work, we obtain for the first time Ag NP films via SCBD directly on the surface of microscope slides, with an easy control over film thickness and density. The films are extremely uniform and composed of pure Ag NPs with an average diameter of 8 nm. Data show that the NP oxidation state is Ag_2O and the films present a high bactericidal activity against a wide range of clinically relevant pathogens (including extensively drug-resistant Gram positive and Gram negative strains).

Methods

NP film synthesis and characterization

Nanostructured Ag films were deposited at room temperature (RT) in medium vacuum (base pressure 1×10^{-6} mbar) conditions by SCBD based on the pulsed microplasma cluster source (see Figure S1 of Supplementary Materials)[18-20] directly on the surface of soda lime glass (SLG) microscope slides (electron microscopy sciences). The nominal film thickness and deposition rate were measured during deposition by a quartz microbalance, while film physical properties where obtained *ex situ* by atomic force microscopy (AFM) (Solver-pro NT-MDT), X-Ray photoemission spectroscopy (XPS), Auger Spectroscopy, X-Ray diffraction (XRD) and optical absorption spectroscopy. Once deposited in the vacuum chamber, the films are extracted to air and either transferred to the measurement apparatus or left exposed to the environment. More details on the experimental characterization procedures can be found in Supplementary Materials.

Antimicrobial activity of Ag NP films

Antimicrobial activity of Ag NP films was investigated against a panel of clinically relevant microorganisms, representative of both Gram negative and Gram positive bacteria, and yeasts. They included six reference strains (i.e. *Escherichia coli* ATCC 25922, *Pseudomonas aeruginosa* PAO-1, *Acinetobacter baumannii* ATCC 17978, *Staphylococcus aureus* ATCC 6538, *Enterococcus faecalis* ATCC 29212, *Candida albicans* ATCC 10231) and ten clinical strains exhibiting antimicrobial resistance phenotypes of concern and/or being recognized as members of high-risk epidemic clones (see Table 1 and references therein[21-27] for clinical strains characteristics).

Antimicrobial activity testing was performed using the procedure proposed by Pallavicini et al,[28] with some minor modifications. Briefly, 1 ml of an overnight culture was washed twice with Phosphate Buffered Saline (PBS) pH 7.4, and 10 μl of microorganism suspension (i.e. range 5.4-7.3 log Colony Forming Units [CFU], see Table T1 of Supplementary Materials for details) was deposited both in a glass slide containing the Ag NP film (challenge slide) and in an unmodified glass slide (control slide), and a glass coverslip was applied (20 × 20 mm). After 24 h of incubation at 25 °C in damp environment, microorganisms were suspended in 10 ml of PBS, appropriately diluted, and 240 μl of each dilution was plated for viable cell count (i.e. enumeration of CFU). The log reduction rate was expressed as Microbicidal Effect (ME), following the formula: $ME = \log N_C - \log N_E$ (where N_C and N_E represented the number of CFU obtained with control slides and challenge slides, respectively). The detection limit of viable cell count was 4.2×10^1 CFU. All microorganisms were tested in three independent experiments and results were averaged. In order to calculate standard deviations (SDs), when no viable cells were counted, the result was arbitrary assumed as 4.2×10^1 CFU, representing the detection limit value. All microorganisms were grown aerobically at 37 °C in a shaker incubator (200 rpm) in Mueller–Hinton II broth (BD, Becton, Dickinson and Company, Sparks, MD, USA), except for *Enterococcus* spp. and *C.*

Table 1
Microbicidal Effect (ME) of Ag NP films against clinically relevant microorganisms after 24 h of exposure.

Strain	ME (log CFU ± SD)	Strain features
Gram negatives		
Escherichia coli ATCC 25922	≥5.6 ± 0.1	Reference strain
Escherichia coli CVB-1	≥5.7 ± 0.1	XDR clinical isolate producing the carbapenemase NDM-1[21]
Klebsiella pneumoniae FIPP-1	5.4 ± 0.4	XDR epidemic ST258 clone producing the carbapenemase KPC-3[22]
Klebsiella pneumoniae KKBO-4	5.2 ± 0.7	XDR epidemic ST258 clone producing the carbapenemase KPC-3 and resistant also to colistin[23]
Pseudomonas aeruginosa PAO-1	≥5.7 ± 0.3	Reference strain
Pseudomonas aeruginosa VR-143/97	2.6 ± 0.8	XDR epidemic clone producing the carbapenemase VIM-1[24]
Acinetobacter baumannii ATCC 17978	4.2 ± 0.1	Reference strain
Acinetobacter baumannii RUH 134	3.9 ± 0.7	Reference strain for the global clone 2[25]
Acinetobacter baumannii AB06C13	4.2 ± 0.5	XDR clinical isolate belonging to global clone 2 and producing the carbapenemases OXA-23 and OXA-58[26]
Gram positives		
Staphylococcus aureus ATCC 6538	3.7 ± 0.8	Reference strain
Staphylococcus aureus MRSA-IT16	4.4 ± 0.4	Methicillin-resistant clinical isolate from biofilm-associated infection[27]
Staphylococcus aureus MRSA-IT1	2.0 ± 0.4	Methicillin-resistant clinical isolate from biofilm-associated infection and exhibiting hVISA and daptomycin resistance phenotype[27]
Enterococcus faecalis ATCC 29212	1.7 ± 0.6	Reference strain
Enterococcus faecium FI2013	0.9 ± 0.2	Glycopeptide-resistant clinical isolate from bloodstream infection
Yeasts		
Candida albicans ATCC 10231	0.7 ± 0.1	Reference strain
Candida albicans EMO1303	1.0 ± 0.1	Clinical isolate from bloodstream infection

CFU, colony forming unit; SD, standard deviation; XDR, extensively drug resistant isolates exhibiting a resistance phenotype including aminoglycosides, fluoroquinolones, and β-lactams (including also carbapenems); hVISA, heterogeneous vancomycin-intermediate *Staphylococcus aureus*.

albicans for which Brain-Heart-Infusion broth (BD) and Yeast Extract-Peptone-Dextrose broth (BD) were used, respectively. Viable cell count was performed in Sabouraud-Dextrose agar (Oxoid, Milan, Italy) for *C. albicans*, and in Luria-Bertani Agar (LBA) (Oxoid) for all other microorganisms.

Results

A representative atomic force microscopy (AFM) image of the as-deposited NP films synthesized in the present work is shown in Figure 1, *A*. The NPs exhibit no signs of fragmentation and present a very homogeneous distribution (rms roughness < 1 nm) with no coarsening over the entire covered area (about 15 cm^2). This is a common feature in SCBD films due to the NP soft landing, regardless of the type of compound deposited.[18,19] The average NP size obtained from the AFM data is around 20 nm (see inset of Figure 1, *A*). However, this has to be taken as an upper limit due to the convolution of the NP shape with the AFM tip (nominal radius 10 nm). X-ray diffraction data (see Figure S2 of Supplementary Materials) indicate that the NPs are partly crystalline and have an average crystallographic domain size of 3.2 ± 0.1 nm, which has to be taken as lower limit (see description of Figure S2 of Supplementary Materials). Since the film thickness measured by AFM is 7.8 ± 0.6 nm and the average height obtained from a statistical analysis of the AFM images is 3.8 (see Figure S3 of Supplementary Materials), it is reasonable to consider an average diameter of 7.8 ± 0.6 nm. Hence the film thickness chosen in the present work corresponds to a single layer of NPs i.e. 8 nm, with an NP density 70 ± 2 NPs on an area of 6.25×10^4 nm^2, i.e. $1.15 \pm 0.04 \times 10^{11}$ NPs/cm^2, as deduced from the AFM data. Since the film density depends on the deposition time, it can be easily tuned from a very low coverage (few percent of the surface area) up to a single layer and beyond.

The chemical state of the NP film has been investigated using XPS and Auger. The Ag Auger line shape is very sensitive to the Ag oxidation state.[29-31] A comparison of normalized MNN Auger spectra, obtained from the 8 nm Ag NP film deposited on the SLG substrate (curve b) and from a polycrystalline, metallic Ag reference (curve a), is shown in Figure 1, *B* together with their difference (curve (b − a)). Spectrum b) presents a broader line shape, reflected in the difference peak at 351 ± 0.5 eV, while the feature at 357 ± 0.5 eV is due to the appearance of a new structure: both consistent with the presence of Ag^+ ions.[31] The oxidation of the as-deposited NP film is confirmed by the XPS data shown in Figure 1, *C*, where the normalized O1s core levels obtained from the as-deposited Ag NPs (curve b) and from the clean SLG substrate (curve a) are shown, together with their difference (curve (b − a)). A least square fitting procedure (see Figure S4 of Supplementary Materials) shows that the clean SLG spectrum presents the SiO_2 peak at 531.6 eV ± 0.5 eV, and a shoulder at 530.1 ± 0.5 eV, due to contributions of Na_2O and CaO.[32] The data taken on the Ag NP film show an intensity increase of the shoulder at 530.1 ± 0.5 eV, due to the appearance of a peak at 530.2 ± 0.5 eV, typical of Ag_2O.[32] Although a possible core-shell structure of NPs with an oxidized shell surrounding a metallic core cannot be ruled out, the data indicate that in the synthesized film the NPs are in a Ag_2O oxidation state. This is a required condition for NPs to release Ag^+ ions, process recently proposed as the more relevant mechanism with respect to the role of the NP size giving rise to the bactericidal activity of the NPs.[8]

Since the typical time elapsed between film synthesis and an antimicrobial activity test was within 15 days, we have analyzed

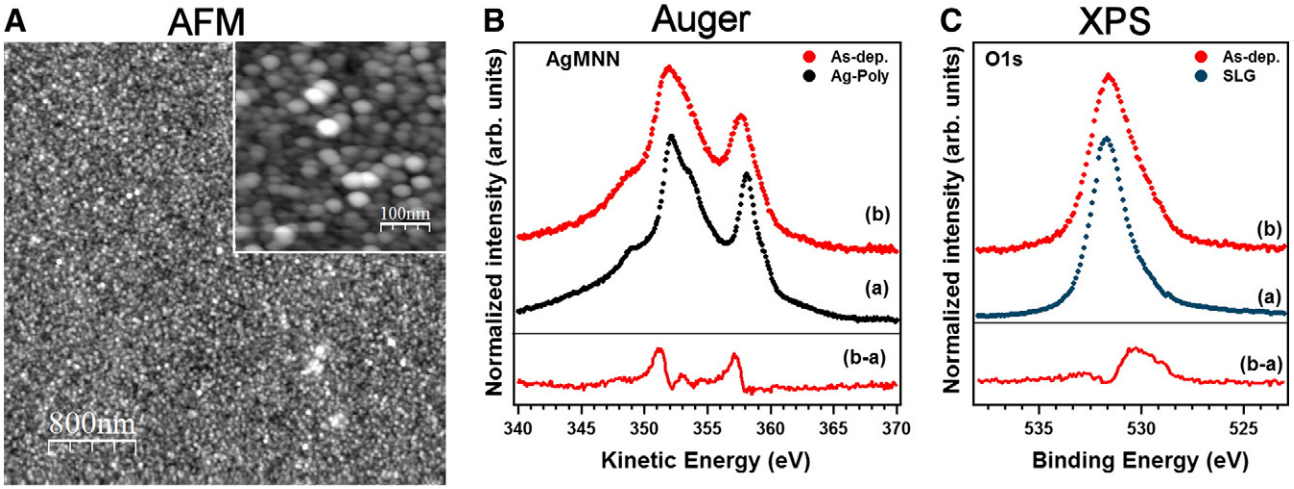

Figure 1. **(A)** AFM image of the as-deposited Ag NP film, showing the uniformity at microscopic scale. Inset: high resolution image where the NP size can be observed. **(B)** Auger spectra of the as-deposited NP film (curve **(b)**, red dots) and metallic polycrystalline Ag reference (curve **(a)**, black dots), with the difference spectrum shown in the bottom to highlight the oxidation state of the NP film. **(C)** XPS spectra of the O1s core level for the as-deposited NP film (curve **(b)**, red dots) and for the clean microscope slide (curve **(a)**, blue dots), with the difference spectrum shown in the bottom to highlight the oxidation state of the NP film.

the NP films as a function of time. After 15 days we observe only a slight increase of the average NP size, as quantified in Figure 2, *C*, showing that the density and the Ag NP size are basically unchanged. In Figure 2, *E* we report the Auger data taken at increasing time intervals that are compared to the as deposited curve through the difference spectra in the bottom panel. We can note only a slight intensity increase of the Ag_2O component, suggesting that just after the synthesis some of the NPs (less than 2% according to the intensity variation) are not completely oxidized. Such increase is also reflected in a sharpening of the plasmon resonance observed in the optical absorption spectra shown in Figure 2, *D*. The broad feature around 480 nm is consistent with the fact that the NPs are in contact with each other, hence giving rise to different resonances related to different NP sizes. The fact that film morphology is not modified as a function of time, in particular the NP diameter, markedly differentiates this type of NP films from previously observed backward/forward reactions observed in colloidal suspensions.[33] The overall emerging picture is that the synthesized films have a very good stability with respect to coarsening and oxidation state.

Ag NP films were found to exert a broad-spectrum bactericidal activity, which was demonstrated both with reference strains and with a collection of clinical strains that exhibited extensively drug-resistant phenotypes and/or belonged to high-risk hyperepidemic clones (see Table 1 and references therein for strains characteristics).[21-27] In particular, after 24 h of exposure to Ag NP films, a reduction of viable bacterial loads by more than 3 log (compared to controls) was observed with 10 of the 14 bacterial strains tested, including representatives of both Gram positive and Gram negative pathogenic species (Tables 1 and T1 of Supplementary Materials). Members of the family Enterobacteriaceae (i.e. *E. coli* and *K. pneumoniae*), which are normal constituents of the intestinal microbiota and among the most common causes of HAIs[12] showed a consistently very high susceptibility to Ag NP films (i.e. ME > 5 log CFU) (Tables 1 and T1 of Supplementary Materials). Interestingly, Ag NP films could almost completely sterilize a high inoculum (i.e. $\sim 1 \times 10^7$ CFU) of extensively drug-resistant clinical strains producing two of the most worrisome resistance mechanisms recently emerged in enterobacteria and capable of pandemic dissemination, such as the carbapenemases NDM-type and KPC-type.[21-23] An overall strong bactericidal activity (i.e. ME range > 5.7-2.6 log CFU) was also demonstrated with reference and clinical strains of *P. aeruginosa* and *A. baumannii*, including representative of extensively drug-resistant high-risk clones (Tables 1 and T1 of Supplementary Materials). Those microorganisms are major opportunistic pathogens in the hospital setting, with a high propensity to evolve extensively drug-resistant and even totally drug-resistant phenotypes and to survive for long periods in the hospital environment (accounting for the occurrence of nosocomial epidemics through, for example, contaminated taps, sinks or even antiseptic solutions).[13] The finding of a lower susceptibility to Ag NP films of the clinical *P. aeruginosa* VR-143/97 strain compared to the other four Gram negative non-fermenters tested, could suggest that this extensively drug-resistant strain might have evolved some resistance mechanism also to Ag NPs (e.g. by chromosomal mutations or horizontal gene transfer). Concerning Gram positive bacteria, high susceptibility to Ag NP films was demonstrated with two of the three *S. aureus* tested (ME > 3 log CFU), including a reference strain and a methicillin-resistant strain isolated from a biofilm-related infection (i.e. naive valve endocarditis) (Tables 1 and T1 of Supplementary Materials). Biofilm-forming bacteria are a major challenge in nosocomial settings, due to their tolerance to antiseptic and antimicrobial agents, and have been estimated to be responsible for more than 60% of HAIs, mainly associated to the presence of artificial medical devices (e.g. mechanical ventilators, central venous catheters, prosthetic devices etc.).[34] The *S. aureus* strain exhibiting a reduced susceptibility to Ag NPs (i.e. ME = 2 log CFU), was also isolated from a biofilm-associated infection (i.e. post-surgical wound infection) and was characterized by an uncommon resistance phenotype extended also to daptomycin (one of the most recent antibiotic class entered the clinical practice). It could be hypothesized that the overall reduction of anionic surface charge

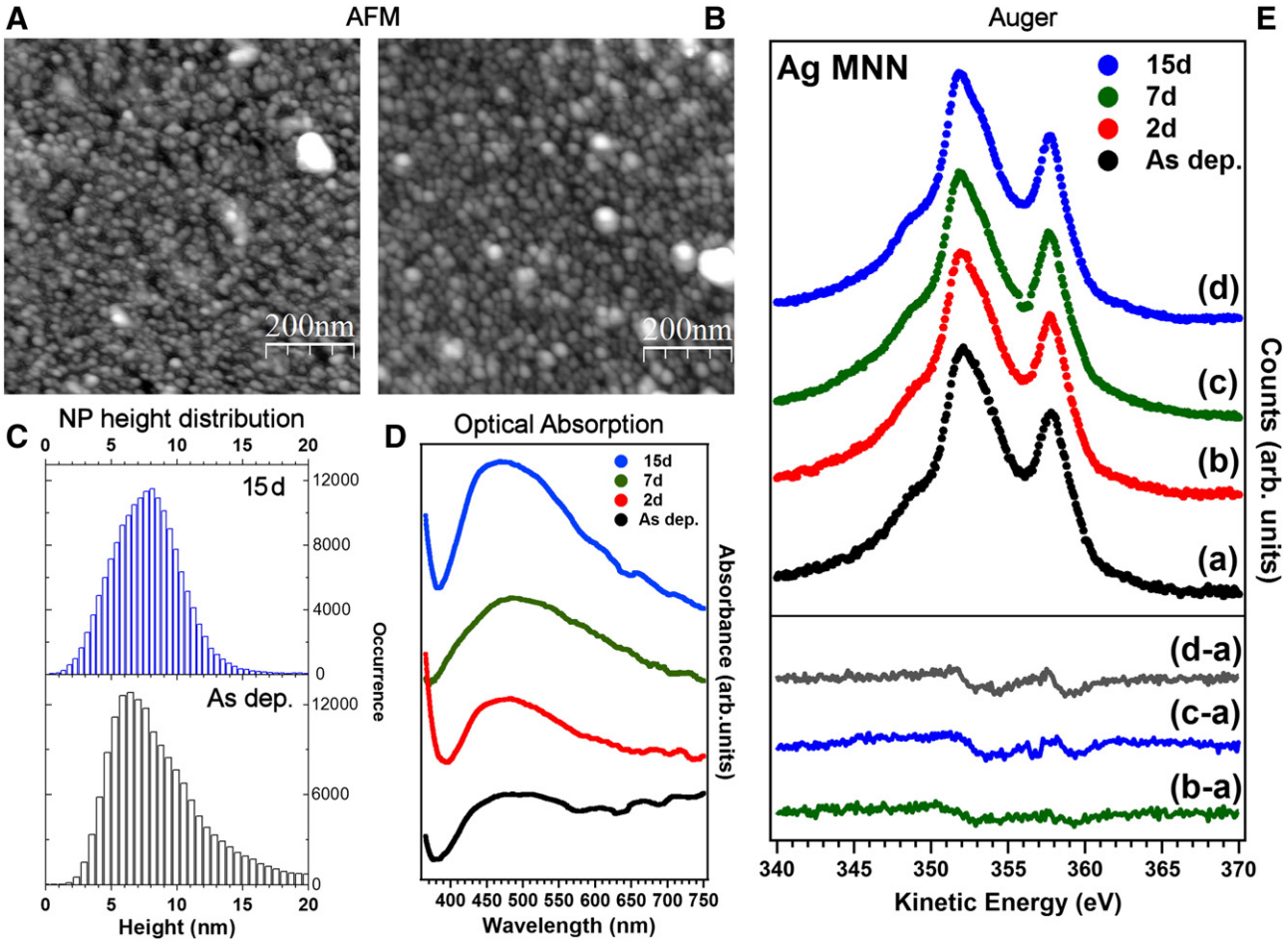

Figure 2. **(A)** AFM image of the as-deposited film; **(B)** AFM image of the same film after 15 days of exposure to air. **(C)** NP height distribution obtained from **(a)** (bottom) and **(b)** (top), respectively. **(D)** Optical absorption spectra as a function of elapsed time after deposition. **(E)** Auger spectra taken at different time intervals, with the difference curves in the bottom panel.

that has been associated to daptomycin resistance in *S. aureus*[35] might have contributed to the reduced susceptibility to Ag NPs, by impairing the interaction with the positively charged silver ions, a fact that would worth further investigation. Finally, *Enterococcus* spp. strains exhibited a relatively low susceptibility to Ag NP films (ME range 0.9-1.7 log CFU), as well as the two *C. albicans* strains (ME range 0.7-1 log CFU) (Tables 1 and T1 of Supplementary Materials). The poor activity of Ag NPs against the latter microorganisms is an intriguing phenomenon, and the reasons accounting for this will deserve further attention. The possibility to use the flexibility of the SCBD for generating NPs with mixed chemical composition will allow investigating antimicrobial features of diverse NP films, with the aim of implementing antimicrobial surfaces which could include also those important nosocomial pathogens.

Discussion

The Ag antimicrobial properties have been known for long time, although the synthesis of Ag NPs as antimicrobial material is relatively recent.[15] This has brought to include Ag NPs in a wide variety of applications[14] but also to propose their use as coatings. However, the transfer from the synthesized NPs from solutions onto the substrate has evidenced the NP coarsening effect and the weak bound formed between the NPs and the substrate.[16,17] Recently, for wet-synthesized Ag NPs transferred on glass, an amino-silanization treatment of the surface has been proposed[17] to increase the adhesion of the coating. The results presented here demonstrate a completely different route to synthesize Ag NPs as compared to the wet chemistry approach. The use of SCBD allows the immediate and direct deposition of the coating on virtually any substrate, with a perfect control over the coating thickness and density that are dependent only on deposition time. Moreover, the synthesis process is completely free of solvents and produces ultrapure Ag NPs, while it does not require any pretreatment or formation of a siloxane sol as mandatory prerequisite to stabilize the Ag NPs obtained by wet chemistry. The film deposited by SCBD on soda lime glass substrates presented here have a good stability also with respect to time (see Figure S5 of Supplementary Materials): it is worth noting that the exposure to air of the SCBD film does not alter its morphology apart from a very slight coarsening of the NPs, while the percent of NPs that are oxidized is even improved. Moreover, the observed film stability with respect to time is comparable to that of the Ag NP films deposited on amino-silanized surfaces as

reported by Taglietti et al.[17] Concerning the film adhesion to the SLG surface, we have compared the behavior of the SCBD films on plane glass and on amino-silanized glass.[17] The adhesion of the film has been tested by employing a home-made scratching test and subsequently measuring the optical transmission of the film, as described in the Supplementary Materials. The main result is that the SCBD film is indeed able to persist after the scratch test, although the presence of the silanization layer improves the wear resistance by about 15 %, as indicated by the intensity variation of the optical transmission (See Figure S5 of Supplementary Materials). These data confirm that on glass the silanization pretreatment is able to improve the adhesion, but is however not necessary in our case to obtain a fairly stable film.

Considering the dimension of the covered area reported in this experiment it is possible to envisage a scalability of this technique to larger surfaces and to surfaces of metals without modification of the proposed synthesis process. It is also worth noting that the SCBD approach has a large development potential in terms of control of the Ag NP surface adhesion through the formation of NPs alloyed with other biocompatible metals. Such potential has been already suggested by synthesis of a 95%–5% Ti–Cr alloy where Cr is located in substitutional sites of the Ti lattice.[19]

As far as the antimicrobial activity is concerned, the effectiveness of the film prepared here is relevant and with a broad spectrum. Indeed, after 24 h of exposure a bactericidal activity (i.e. decrease in viable cell count $\geq$99.9%) was observed with most tested bacterial strains, including representatives of the major clinically relevant Gram negative and Gram positive pathogens. The notable lower antimicrobial activity of the Ag NP films obtained in this study against *Enterococcus* spp. and *C. albicans*, and the observation of reduced susceptibility in some extensively drug-resistant *P. aeruginosa* and *S. aureus* clinical strains, represent a limitation that will be addressed in future studies through the implementation of NP films with mixed chemical composition.

In perspective, the ability to modify the NP chemical composition provided by the SCBD method will open large possibilities for tailoring the active material in order to: optimize the precious metal amount; expand the spectrum of antimicrobial activity; reduce the risk for resistance development; tailor the adhesion to surfaces to obtain a long lasting, low cost antimicrobial film, in particular for metal surfaces.

In conclusion we have demonstrated the realization of a uniform Ag NP film with extremely controlled thickness and NP size directly on a substrate surface through a simple and scalable technique, SCBD. The Ag_2O oxidation state of the NPs and the film morphology are stable in time. We have demonstrated that such films present a relevant and broad-spectrum bactericidal activity that could be related to the oxidation state of the Ag NPs. This work opens the way for exploring the potential of supersonic beams as alternative method for antibacterial coating synthesis.

Acknowledgement

We thank Mirco Chiodi for performing XRD measurements.

Appendix A. Supplementary data

Supplementary data to this article can be found online at http://dx.doi.org/10.1016/j.nano.2015.02.023.

References

1. Boisselier E, Astruc D. Gold nanoparticles in nanomedicine: preparations, imaging, diagnostics, therapies and toxicity. *Chem Soc Rev* 2009;**38**:1759-82.
2. Liu C, Burghaus U, Besenbacher F, Wang ZL. Preparation and characterization of nanomaterials for sustainable energy production. *ACS Nano* 2010;**4**:5517-26.
3. Li Q, Mahendra S, Lyon DY, Brunet L, Liga MV, Li D, et al. Antimicrobial nanomaterials for water disinfection and microbial control: potential applications and implications. *Water Res* 2008;**42**:4591-602.
4. Badireddy AR, Hotze EM, Chellam S, Alvarez PJJ, Wiesner MR. Inactivation of bacteriophages via photosensitization of fullerol nanoparticles. *Environ Sci Technol* 2007;**41**:6627-32.
5. Seil JT, Webster TJ. Antimicrobial applications of nanotechnology: methods and literature. *Int J Nanomedicine* 2012;**7**:2767-81.
6. Tolaymat TM, El Badawy AM, Genaidy A, Scheckel KG, Luxton TP, Suidan M. An evidence-based environmental perspective of manufactured silver nanoparticle in syntheses and applications: a systematic review and critical appraisal of peer-reviewed scientific papers. *Sci Total Environ* 2010;**408**:999-1006.
7. Seo YI, Hong KH, Kim DG, Kim YD. $Ag/Al(OH)_3$ mesoporous nanocomposite film as antibacterial agent. *Colloids Surf B Biointerfaces* 2010;**81**:369-73.
8. Xiu ZM, Zhang QB, Puppala HL, Colvin VL, Alvarez PJJ. Negligible particle-specific antibacterial activity of silver nanoparticles. *Nano Lett* 2012;**12**:4271-5.
9. Guzman M, Dille J, Godet S. Synthesis and antibacterial activity of silver nanoparticles against gram-positive and gram-negative bacteria. *Nanomedicine* 2012;**8**:37-45.
10. Boucher HW, Talbot GH, Bradley JS, Edwards JE, Gilbert D, Rice LB, et al. Bad bugs, no drugs: no ESKAPE! An update from the Infectious Diseases Society of America. *Clin Infect Dis* 2009;**48**:1-12.
11. Weber DJ, Rutala WA. Self-disinfecting surfaces: review of current methodologies and future prospects. *Am J Infect Control* 2013;**41**:S31-5.
12. European Centre for Disease Prevention and Control. Point prevalence survey of healthcare-associated infections and antimicrobial use in European acute care hospitals 2011-2012. http://www.ecdc.europa.eu/en/publications/Publications/healthcare-associated-infections-antimicrobial-use-PPS.pdf2013.
13. Weber DJ, Anderson D, Rutala WA. The role of the surface environment in healthcare-associated infections. *Curr Opin Infect Dis* 2013;**26**:338-44.
14. Chaloupka K, Malam Y, Seifalian AM. Nanosilver as a new generation of nanoproduct in biomedical applications. *Trends Biotechnol* 2010;**28**:580-8.
15. Rycenga M, Cobley CM, Zeng J, Li W, Moran CH, Zhang Q, et al. Controlling the synthesis and assembly of silver nanostructures for plasmonic applications. *Chem Rev* 2011;**111**:3669-712.
16. Yliniemi K, Vahvaselka M, Van Ingelgem Y, Baert K, Wilson BP, Terryn H, et al. The formation and characterisation of ultra-thin films containing Ag nanoparticles. *J Mater Chem* 2008;**18**:199-206.
17. Taglietti A, Arciola CR, D'Agostino A, Dacarro G, Montanaro L, Campoccia D, et al. Antibiofilm activity of a monolayer of silver nanoparticles anchored to an amino-silanized glass surface. *Biomaterials* 2014;**35**:1779-88.
18. Barborini E, Kholmanov IN, Piseri P, Ducati C, Bottani CE, Milani P. Engineering the nanocrystalline structure of TiO2 films by aerodynamically filtered cluster deposition. *Appl Phys Lett* 2002;**81**:3052-4.
19. Chiodi M, Parks Cheney C, Vilmercati P, Cavaliere E, Mannella N, Weitering HH, et al. Enhanced dopant solubility and visible-light absorption in Cr-N co-doped TiO_2 nanoclusters. *J Phys Chem C* 2012;**116**:311-8.

20. Chiodi M, Cavaliere E, Kholmanov IN, de Simone M, Sakho O, Cepek C, et al. Nanostructured TiO_x film on Si substrate: room temperature formation of $TiSi_x$ nanoclusters. *J Nanopart Res* 2010;**12**:2645-53.
21. D'Andrea MM, Venturelli C, Giani T, Arena F, Conte V, Bresciani P, et al. Persistent carriage and infection by multidrug-resistant *Escherichia coli* ST405 producing NDM-1 carbapenemase: report on the first Italian cases. *J Clin Microbiol* 2011;**49**:2755-8.
22. Giani T, D'Andrea MM, Pecile P, Borgianni L, Nicoletti P, Tonelli F, et al. Emergence in Italy of *Klebsiella pneumoniae* sequence type 258 producing KPC-3 carbapenemase. *J Clin Microbiol* 2009;**47**:3793-4.
23. Cannatelli A, D'Andrea MM, Giani T, Di Pilato V, Arena F, Ambretti S, et al. *In vivo* emergence of colistin resistance in *Klebsiella pneumoniae* producing KPC-type carbapenemases mediated by insertional inactivation of the PhoQ/PhoP *mgrB* regulator. *Antimicrob Agents Chemother* 2013;**57**:5521-6.
24. Riccio ML, Pallecchi L, Docquier JD, Cresti S, Catania MR, Pagani L, et al. Clonal relatedness and conserved integron structures in epidemiologically unrelated *Pseudomonas aeruginosa* strains producing the VIM-1 metallo-beta-lactamase from different Italian hospitals. *Antimicrob Agents Chemother* 2005;**49**:104-10.
25. Diancourt L, Passet V, Nemec A, Dijkshoorn L, Brisse S. The population structure of *Acinetobacter baumannii*: expanding multiresistant clones from an ancestral susceptible genetic pool. *PLoS One* 2010;**5**:e10034.
26. Principe L, Piazza A, Giani T, Bracco S, Caltagirone MS, Arena F, et al. Epidemic diffusion of OXA-23-producing *Acinetobacter baumannii* isolates in Italy: results of the first cross-sectional countrywide survey. *J Clin Microbiol* 2014;**52**:3004-10.
27. Landini L, Riccobono E, Giani T, Arena F, Rossolini GM, Pallecchi L. Bactericidal activity of ceftaroline against mature *Staphylococcus aureus* biofilms. *Int J Antimicrob Agents* 2015, http://dx.doi.org/10.1016/j.ijantimicag.2015.01.001.
28. Pallavicini P, Taglietti A, Dacarro G, Diaz-Fernandez YA, Galli M, Grisoli P, et al. Self-assembled monolayers of silver nanoparticles firmly grafted on glass surfaces: low Ag^+ release for an efficient antibacterial activity. *J Colloid Interface Sci* 2010;**350**:110-6.
29. Waterhouse GIN, Bowmaker GA, Metson JB. Oxidation of a polycrystalline silver foil by reaction with ozone. *Appl Surf Sci* 2001;**183**:191-204.
30. Wagner CD. Auger lines in x-ray photoelectron spectrometry. *Anal Chem* 1972;**44**:967-73.
31. Giallongo G, Pilot R, Durante C, Rizzi GA, Signorini R, Bozio R, et al. Silver nanoparticle arrays on a DVD-derived template: an easy & cheap SERS Substrate. *Plasmonics* 2011;**6**:725-33.
32. Miura Y, Kusano H, Nanba T, Matsumoto S. X-ray photoelectron spectroscopy on sodium borosilicate glasses. *J Non-Cryst Solids* 2001;**290**:1-14.
33. Douglas Gallardo OA, Moiraghi R, Macchione MA, Godoy JA, Perez MA, Coronado EA, et al. Silver oxide particles/silver nanoparticles interconversion: susceptibility of forward/backward reactions to the chemical environment at room temperature. *RSC Adv* 2012;**2**:2923-9.
34. Costerton JW, Stewart PS, Greenberg EP. Bacterial biofilms: a common cause of persistent infections. *Science* 1999;**284**:1318-22.
35. Humphries RM, Pollett S, Sakoulas G. A current perspective on daptomycin for the clinical microbiologist. *Clin Microbiol Rev* 2013;**26**:759-80.